STIFFNESS AND FORCE IN ACTIVATED FROG SKELETAL MUSCLE FIBERS

GIOVANNI CECCHI, PETER J. GRIFFITHS, AND STUART TAYLOR
Department of Pharmacology, Mayo Foundation, Rochester, Minnesota 55905

ABSTRACT Single fibers, isolated intact from frog skeletal muscles, were held firmly very near to each end by stiff metal clasps fastened to the tendons. The fibers were then placed horizontally between two steel hooks inserted in eyelets of the tendon clasps. One hook was attached to a capacitance gauge force transducer (resonance frequency up to ~50 kHz) and the other was attached to a moving-coil length changer. This allowed us to impose small, rapid releases (complete in <0.15 ms) and high frequency oscillations (up to 13 kHz) to one end of a resting or contracting fiber and measure the consequences at the other end with fast time resolution at 4 to 6°C. The stiffness of short fibers (1.8–2.6 mm) was determined directly from the ratio of force to length variations produced by the length changer. The resonance frequency of short fibers was so high (~40 kHz) that intrinsic oscillations were not detectably excited. The stiffness of long fibers, on the other hand, was calculated from measurement of the mechanical resonance frequency of a fiber. Using both short and long fibers, we measured the sinusoids of force at one end of a contracting fiber that were produced by relatively small sinusoidal length changes at the other end. The amplitudes of the sinusoidal length changes were small compared with the size of step changes that produce nonlinear force-extension relations. The sinusoids of force from long fibers changed amplitude and shifted phase with changes in oscillation frequency in a manner expected of a transmission line composed of mass, compliance, and viscosity, similar to that modelled by (Ford, L. E., A. F. Huxley, and R. M. Simmons, 1981, *J. Physiol. (Lond.)*, 311:219–249). A rapid release during the plateau of tetanic tension in short fibers caused a fall in force and stiffness, a relative change in stiffness that putatively was much smaller than that of force. Our results are, for the most part, consistent with the cross-bridge model of force generation proposed by Huxley, A. F., and R. M. Simmons (1971, *Nature (Lond.)*, 213:533–538). However, stiffness in short fibers developed markedly faster than force during the tetanus rise. Thus our findings show the presence of one or more noteworthy cross-bridge states at the onset and during the rise of active tension towards a plateau in that attachment apparently is followed by a relatively long delay before force generation occurs. A set of equations is given in the Appendix that describes the frequency dependence of the applied sinusoid and its response. This model predicts that frequency-dependent changes can be used as a measure of a change in stiffness.

INTRODUCTION

In the model of Huxley and Simmons (1971), force generation in skeletal muscle occurs as a result of the rotation of attached cross-bridge heads. When attached cross-bridges rotate, they stretch an associated elastic element through which force is transmitted between the thick and thin filaments. In the absence of significant compliance from the tendons or from the filaments, this elasticity is the principal source of compliance in a muscle fiber. Therefore, the instantaneous stiffness of a muscle can be used as one of the methods to assess the degree of cross-bridge attachment under different experimental conditions (Huxley and Simmons, 1972). Huxley and Simmons (1971; 1972) attributed the first few milliseconds of force recovery that follows a stepwise decrease in the length of a contracting fiber to relatively fast rotation of attached cross-bridge heads, and the early part of force recovery putatively occurs without net attachment or detachment of cross-bridges.

We measured instantaneous stiffness of short muscle fibers (~2 mm) to determine whether the recovery from a step length change occurs without net change in the number of attached cross-bridges, as predicted by Huxley and Simmons (1971), or whether stiffness during the quick recovery is more consistent with other models that contain a different mixture of modifications to A. F. Huxley's 1957 model, modifications made necessary by the discovery of transient responses to sudden changes in length or load (e.g., Podolsky and Nolan, 1972). Data reported by Julian and Morgan (1981) and Ford et al. (1974) with somewhat longer fibers (5–6 mm) indicate that the change in stiffness after a step change in fiber length is much smaller than the change in force, which data is consistent with the theory of

Dr. Griffiths' present address is University Laboratory of Physiology, Oxford, United Kingdom.

Dr. Cecchi's present address is Department of Physiology, University of Florence, Italy.

Address correspondence to Stuart Taylor, Ph.D., Department of Pharmacology, Mayo Foundation, 711 Guggenheim, Rochester, MN 55905.

Huxley and Simmons (1972). The precise time course of these changes in stiffness during the quick recovery from a fast length step has not yet been described with the resolution of our measurements, and we found large amounts of apparent cross-bridge detachment after fast steps. However, we believe this is not a true indication of cross-bridge detachment for two reasons: (*a*) our force-extension measurements showed a close relationship between these variables during release and tension recovery; (*b*) the stiffness of short fibers measured directly by high frequency oscillations during slower releases differed only slightly from the stiffness at the same tension during the quick recovery.

Previous measurements of instantaneous stiffness show a constant stiffness-to-force ratio at different force levels when the force of a skeletal muscle fiber is varied as a function of either the sarcomere length (Huxley and Simmons, 1972; Ford et al., 1981) or the activating free calcium concentration (Yamomoto and Herzig, 1978). Stiffness measurements during rapid activation of skinned muscle fibers also suggest a constant stiffness-to-force ratio during the earliest stage of activation (Griffiths et al., 1979). The skinned fibers experiments obviously did not precisely duplicate the conditions under which a train of action potentials leads to the rise of tetanic force. Huxley and Simmons (1972) report that stiffness during the tetanus rise increases in proportion to force, but our inspection of the data obtained by Bressler and Clinch (1974) with whole muscle suggested that stiffness during the tetanus rise might be higher than expected.

We have used apparatus with a time resolution that allowed us to make very rapid length changes and record the resulting changes in force of isolated muscle fibers. Stiffness was measured at various times during the tetanus rise and during the plateau to determine if stiffness and force increased at the same rate, which should make the stiffness-to-force ratio constant at each instant. Our data showed a marked lead of the stiffness increase over force. This may reflect the presence of a cross-bridge state not previously resolved in single intact cells with small extrinsic compliance. Cross-bridge attachment is evidently followed by a relatively long delay before force generation as a muscle cell is transformed via the normal mechanisms of excitation from the resting state to a fused steady state of active force generation. Graded depolarization of these muscle cells under conditions in which action potential spread was impaired also caused an inconstant ratio of stiffness to force during the rise of tension. Preliminary reports of some of our results have already appeared (Cecchi et al., 1981*a*, *b*, and 1982*a*, *b*, *c*).

METHODS

Preparation and Protocol

Muscle fiber preparations of three different lengths were used. The length depended on the procedure followed to measure the stiffness. Short fibers (1.8–2.6 mm) isolated from lumbricalis" digiti IV muscles of the frog *Rana temporaria* were used when we wanted to avoid artifacts from mechanical resonance and measure stiffness directly as the ratio between sinusoidal force and length changes. Tibialis anterior fibers (4–7 mm) were also used in some experiments. Long fibers (9–17 mm) isolated from semitendinosus or iliofibularis muscles were used when we wanted to calculate stiffness of a fiber from its resonance frequency obtained experimentally. The frogs were cold-adapted (5°C or less for from at least several weeks to several months before use). Special care was taken during dissection to remove all extracellular material from both ends of the muscle cell and make the points of attachment to each tendon clearly visible. Aluminum clasps or steel wires were attached to the tendons at a distance <50 μm from each end of the cell to minimize tendon compliance. Fibers were then mounted between a capacitance force transducer and a length step generator with either the clasps or wires as attachments. We adjusted the average striation spacing to ~2.2 μm by observing the diffraction pattern of the fibers produced by a 0.5 mW He-Ne laser (Model 155; Spectra-Physics Inc., Autolab Div., Santa Clara, CA). Maximum and minimum values of fiber diameter and total fiber length exclusive of the tendons were measured by light microscopy. The solution in the experimental chamber was kept at a temperature of between 4 and 6 ± 0.5°C by Peltier elements in the microscope stage. Fibers were tetanically stimulated by brief (1 ms) electrical field pulses applied for 600 ms at regular 5-min intervals by way of platinum plate electrodes that extended parallel to the fiber along the whole length of the chamber. The stimulus frequency (usually between 10 and 20 Hz) was adjusted to give a just fused tetanus, and the stimulus intensity was three times the rheobase. At the beginning of each experiment a plot of the extreme force (T_1) reached after steps of different sizes (i.e., a T_1 curve [Huxley and Simmons, 1971]) was constructed for the preparation by means already described (Cecchi et al., 1982*c*). When the extrapolated value of the amount of instantaneous shortening that was required to just bring the force to zero was >0.65% of fiber length, the fiber was not used for these experiments. This criterion was not applied to long fibers in which there was a relatively large influence of fiber inertia. Data obtained during the experiment were stored on magnetic disks after display on a Nicolet Series 2090 Explorer digital oscilloscope (Nicolet Instrument Corporation, Madison, WI). This digital oscilloscope allowed us to perform simple arithmetical manipulations of the data obtained, such as those shown in Fig. 1, with records from a short fiber.

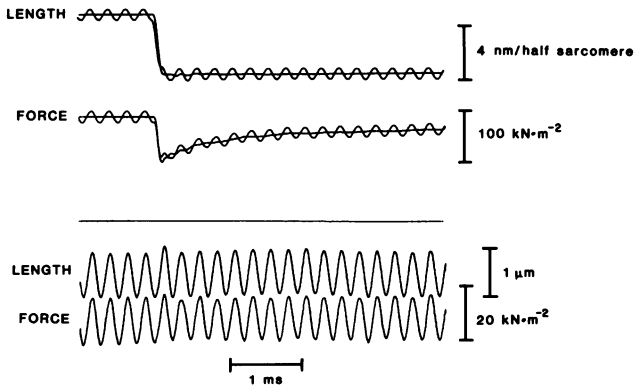

FIGURE 1 The time course of change in force in response to a sudden change of length. The top trace shows two releases imposed during the plateau of a tetanus. Oscillations of 4 kHz were imposed on one end of the fiber in one of the records. The middle trace shows the drop in force and subsequent recovery during releases with and without the oscillations. The straight line indicates the base line of force before and after each tetanus. The bottom two traces show the length and force records after subtractions of the steps without imposed oscillations. This fiber is the same one shown in Fig. 5 and the conditions are the same.

Length Step Generator and Force Transducer

The length step generator was an improved version of a system already described (Cecchi et al., 1976). It consisted of a low inertia moving coil to which a carbon fiber rod 10 cm long was attached. The rod extended into the experimental chamber. A small steel hook was glued to the end of the rod. The position of the coil was signalled by a flag situated between a photodiode (model PN3; Quantrad Corporation, Torrance, CA) and a light source. The light source, photodiode, and flag were enclosed in a light-tight housing to allow us to also monitor aequorin luminescence in separate experiments (e.g., Cecchi et al., 1981*a*). But this required several additional centimeter extensions of the carbon fiber rod and contributed to the deviation between photodiode output and movement of the hook during high frequency sinusoids of length. The output from the photodiode was recorded as a length signal and used as the feedback signal to improve the characteristics of the system. The minimum step time was ~125 μs (e.g., Cecchi et al., 1982*c*; and Fig. 1), the highest usable sinusoidal frequency was 13 kHz and the noise was <0.1 μm peak to peak.

For sinusoidal oscillations at frequencies from 3 to 13 kHz, the movement of the steel hook was not always exactly equal to the output from the photodiode. We observed a small frequency-dependent deviation that ranged from 0 to 20%. Presumably this is because the coil, carbon fiber rod, and hook are not a pure translational mass; the parts cannot be connected together so rigidly that they move only in the "x" direction with identical or proportional velocities and accelerations at all times. For this reason the system was calibrated at the end of each experiment and the photodiode signals were corrected in accordance with this calibration. We measured the real movement of the tip of the carbon fiber by using the hook as a moveable plate of a capacitor and recorded the capacitance changes produced by the movement at each frequency using the electronics of the force transducer. There was no detectable difference between movement of the hook and the photodiode output at the end of a step length change, and no correction was necessary in this case. Therefore, the calibrating bars in Figs. 1 and 6 showing length step changes with superimposed oscillations are more accurate for the length steps than the length sinusoids. The amplitude of the imposed length sinusoid was equal to or greater than the sinusoid that (up to 20%) appears on the trace, depending on the frequency.

The force developed by the fiber was measured by a capacitance gauge transducer of the type described by Huxley and Lombardi (1980). Briefly, the transducer was made of two metallized quartz plates clamped together by springs. The two plates were separated by a small air gap (6–8 μm) obtained by inserting two small pieces of gold foil of this thickness between the plates. A small aluminum lever, terminated by a hook for the attachment of the clasps or the wires, was glued to the middle of the moveable plate. The plates were frequently dismantled to clean and dry the surfaces or re-glue the hook. The characteristics were sometimes changed by these procedures. Occasionally a different transducer was used while another was being refurbished. The resonance frequency of the different transducers used varied between 30 and 50 kHz; their sensitivity varied between 44 and 88 mV/mN and the compliance was ~0.05 μm/mN. The capacitance changes produced by a force applied to the moveable plate were detected by a modified Foster-Seeley phase detector (Cecchi, 1983) similar to the type described by Cambridge and Haines (1959). The detector was set to work at a fixed frequency of 8 MHz. The rise time of the discriminator was <5 μs and the noise <200 μV peak to peak. The discriminator was completely solid state and small enough to be placed very close to the transducer.

Analysis of Results

Force records obtained during the experiment were converted to tension by using the maximum and minimum diameters of the fiber to calculate cross-sectional area, assuming an elliptical shape of the fiber cross section. Length changes were expressed as nanometers per half sarcomere, on the assumptions that (*a*) the fraction of the length change occurring at the tendons was very small and that (*b*) the length change was uniform along the fiber.

Direct measurements of stiffness in short fibers were made by applying sinusoidal length changes and calculating the ratio of the peak amplitude of tension and length sinusoids from records like those shown in Fig. 1. Kawai (1982) has already reviewed the applicability of sinusoidal length changes as a method of measuring cross-bridge kinetics. Dimensionless stiffness values (S) were obtained according to the formula

$$S = \frac{\Delta P}{P_0} \cdot \frac{l_0}{\Delta l}, \tag{1}$$

where P_0 is the active tension during the plateau of a tetanus, ΔP is the peak to peak amplitude of a sinusoid of force per unit cross-section of fiber area recorded at the force transducer end, l_0 is the total length of fiber excluding metal tendon clasps, and Δl is the peak to peak amplitude of a sinusoid length recorded from the photodiode inside the sealed housing of the length step generator.

At the plateau level for developed force or when the force was changing slowly, mean stiffness values were calculated for five cycles. Amplitudes of sinusoidal length changes were adjusted to make each stretch or release less than 0.0005 times the fiber length in order to remain on the linear region of fiber stiffness and to avoid detachment of cross-bridges (Kawai and Brandt, 1980). Neither the amplitude nor time course of tension or tension transients was altered by the application of these sinusoidal length changes.

The stiffness of long fibers was measured indirectly. First, the resonance frequency was measured, then stiffness was calculated on the assumption that viscous forces did not affect the measurements. This method has the advantage that a very fast length change can be used to measure the stiffness because the inertia of the fiber is included in the measure itself. For this reason, this method can be used with long fibers in which the contribution of the tendon compliance to the total compliance is smaller than in a short fiber. To find the resonance frequency, a series of sinusoidal length changes at frequencies between 1 and 13 kHz were applied to one end of the fiber and the corresponding force was recorded at the other end. We defined the resonance frequency as the value at which the phase shift between length and force was $-90°$ and the sinusoidal force output was maximum.

Fiber Length as a Factor in Direct and Indirect Estimates of Stiffness

The mechanical behavior of a stimulated muscle fiber subjected to a rapid length change can be described by a distributed model involving only mass and compliance in the simplest case (Schoenberg et al., 1974). The transmission of force through a fiber resulting from a stretch or a release occurs at a finite speed. Thus, there is a significant delay between the application of the length change and the appearance of the associated force response at the other end of the fiber. In the absence of significant internal damping, this transmission time is given by

$$\text{transmission time} = \frac{\ell_0}{(E/D)}, \tag{2}$$

where E is Young's modulus and D the fiber density.

The resonance frequency (f_n) of the model from which stiffness of a fiber can be calculated is given by

$$f_n = \frac{(E/D)^{1/2}}{2\ell_0}. \tag{3}$$

The mechanical properties of a muscle fiber provide an upper limit to the oscillation frequency that can be used for direct measurements of stiffness because at frequencies of oscillation (f) approaching f_n there is a

significant contribution to the force response owing to the inertia of the fiber. On the other hand, a lower limit to the oscillation frequency is imposed by the speed of the quick recovery of tension, which tends to reduce the size of the force transient accompanying the length change.

It is clear from Eq. 3 that f_n is inversely proportional to fiber length, while the rate of the intrinsic tension recovery mechanism is not (see Blangé et al., 1972, and the accompanying discussion of Huxley and Simmons). Therefore, by using a short preparation such as a fiber from the lumbricalis" digiti IV muscle of the frog, we were able to apply high frequencies of sinusoidal oscillation in direct measurements of stiffness and, thereby, reduce truncation of recorded force by the quick tension recovery mechanism.

RESULTS

Effects of Sinusoidal Length Changes on Force Responses of Long Fibers

To evaluate the steady-state transmission characteristics of our system, we shall first describe the results obtained when a range of sinusoidal oscillation frequencies was imposed on long single fibers. Long fibers (9–12 mm) were selected for these measurements to allow us to excite the resonance frequency, which was not possible with short fibers and a maximum driven frequency of 13 kHz. The accompanying force responses and phase shift between force and length sinusoids were recorded, and the data obtained during the plateau of a series of tetani from one fiber are shown in Fig. 2. The black circles show the values for sinusoids of force, and the crosses indicate the phase angles between the force and the length sinusoids. Note that force responses increase as the frequency increases. Force is maximum at a resonance frequency in which the phase shift is −90°. At low frequencies, force oscillations led length changes. But as the frequency of the driven oscillations increased, force began to lag behind the length changes. At points obtained beyond the resonance frequency, the amplitude of the sinusoids of force began to fall but the phase lag continued to increase. The points obtained in the range 0.1 to 0.4 f_n did not show a marked change in force amplitude. Beyond this range, however, the force and the phase angle increased rapidly.

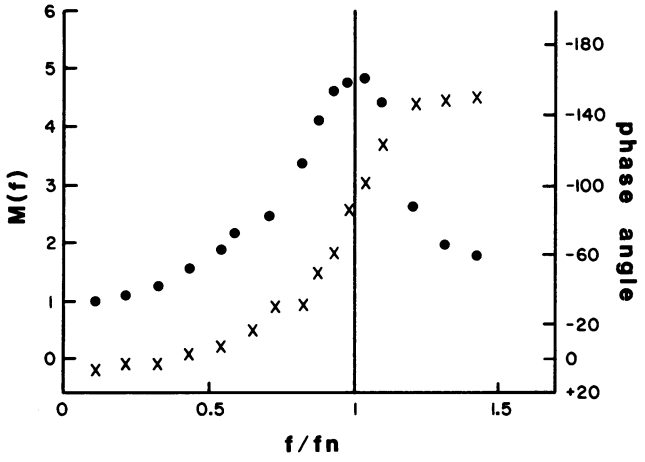

FIGURE 2 The frequency dependence of force responses to small amplitude sinusoidal length changes applied at one end of a long single muscle fiber during tetanic contractions. This fiber was isolated from the iliofibularis muscle (20.i.82). Mechanical amplification ($M[f]$, ●) is equal to the ratio of amplitudes of force sinusoids at 1 kHz to the amplitudes at higher frequencies; phase angle (X) indicates the difference between length oscillations and force records. Frequency is expressed as a ratio of the driven frequency (f) and the resonance frequency (f_n). The resonance frequency of this fiber (f_n), i.e., the frequency at which a 90° phase shift occurred, was only 9.5 kHz. The transmission time along the fiber before a length step could be detected at the force transducer was 48 μs. This leads one to expect a resonance frequency of 10.4 kHz. The difference between this value and that observed experimentally is probably due to damping. Changes in force fell behind length changes as the frequency was increased. Hence, the value of the phase angle became negative in a sigmoidal manner. The temperature was 4°C, fiber length 11.0 mm, and striation spacing 2.2 μm.

The graphs in Figs. 2 and 11 were obtained by measuring the force and length sinusoids some milliseconds after the application of the oscillations, once the steady state was attained. At the onset, immediately after the application of the sinusoidal length changes, the first few force oscillations did not conform to the steady-state behavior of the preparation. This can be seen in Fig. 3. The first few force oscillations differed from the later ones both in amplitude and in phase angle. The transmission time predicted by Eq. 2 was apparent in the records as a delay (~50 μs) between the initiation of the first length cycle and the first force response, and was almost independent of the driving frequency. The later steady-state phase shift between force and length oscillations was shorter and frequency dependent.

Fiber Stiffness Measured by Steps and Oscillations of Short Fibers

The results obtained from imposing sinusoids of length primarily to short fibers are described in the remainder of this section. Although the Huxley and Simmons method of describing fiber stiffness is the T_1 curve obtained using step length changes, the method of using sinusoidal length changes has the advantage of providing a continuous record of fiber stiffness under conditions during which force is changing. Records from a short fiber subjected to oscillation frequencies of 1 to 9 kHz during the tetanus plateau and during the tetanus rise are shown in Fig. 4. The results obtained by analysis of Fig. 4 are reported in Table I. The stiffness measured as the ratio of force to length was frequency-dependent and increased by a factor of about 1.35 between 1 and 4 kHz. From 4 to 9 kHz, the increase was about 1.1 times, whereas the increase was much larger at these frequencies with long fibers (e.g., Figs. 2, 3, and 11). In the lower frequency range, a small phase lead of the force over length was always present. Three factors can account for the increase in stiffness observed with the increase in oscillation frequency. The first one is the quick tension recovery that tends to decrease the stiffness measured at low frequency oscillations. The second possibility is viscosity, and the third one is mechanical amplification

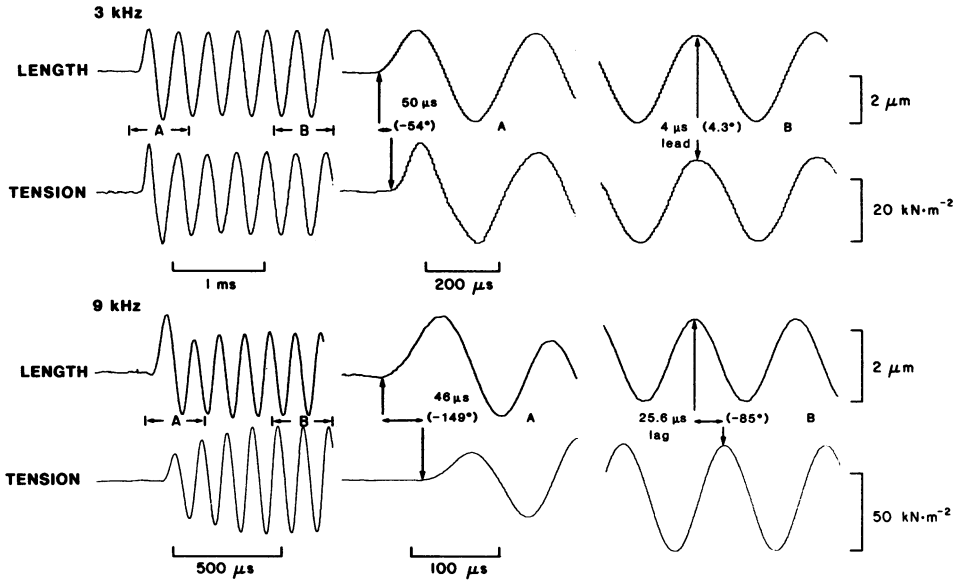

FIGURE 3 Records of force and length oscillations immediately after the application of the oscillations (*A*) and at the steady state (*B*) at two frequencies (3 kHz, upper trace; 9 kHz, lower trace). The eight traces on the right show regions *A* and *B* on a faster time base. Note that the transmission time, shown as a delay between the length and the force sinusoids at the start of the oscillations (*A*), is almost independent of the frequency. At the steady state (*B*), the phase shift between length and force sinusoids is strongly frequency dependent. The same fiber and conditions described in Fig. 2.

of the force output due to the resonance of the fiber. The value of the stiffness found at 9 kHz agrees well with the value expected in the absence of recovery (Ford et al., 1977), although some mechanical amplification could be present at 9 kHz even for this fiber (Table I).

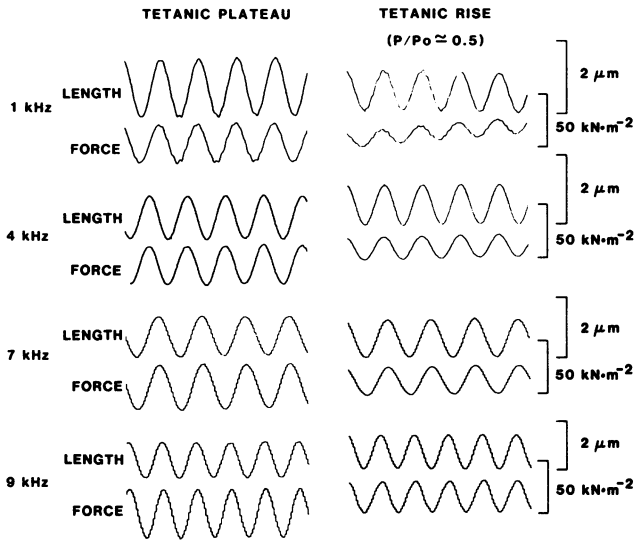

FIGURE 4 Force and length records from an experiment (9.vii.81) in which sinusoidal length changes at four different frequencies were imposed on the tetanic plateau (left) and during the rise of tetanic force (right). The values of fiber stiffness obtained from these records are given in Table I. The steps on some of the records resulted from the relatively long dwell time (5 μs) used on the digital oscilloscope, whereas the analog signals were smooth. This fiber was isolated from the lumbricalis" digiti IV, and was 2.53 mm long at the striation spacing (2.25 μm) and temperature (4°C) of the experiment.

At an oscillation frequency of 4 kHz the mean value of the extrapolated intercept for zero force ("y_0") determined as previously described (Cecchi et al., 1982*c*) was 5.48 nm per half sarcomere (range 4.6 to 6.2) for six short fibers. T_1 curves were also obtained for the fiber of Fig. 4 and several measured and calculated parameters are reported in Table I to compare results with the two methods of measuring fiber stiffness. The T_1 curve for the tetanus plateau of this toe muscle fiber was very similar to that obtained by Ford et al. (1977) with an anterior tibial muscle fiber at a similar temperature (see Fig. 32 of Ford et al., 1977). Their spot follower technique (Ford et al., 1977) avoids any influence of tendon compliance on the T_1 curve. Hence, the contribution of tendon elasticity to the stiffness of our preparations was probably small (for example the "y_0" values in Table I). The extrapolated intercept for zero force obtained from the T_1 curve of this particular fiber was 5.2 nm per half sarcomere. The stiffness of the preparation estimated from the extrapolated intercept of the T_1 curve was similar to the value measured using 4 kHz sinusoidal oscillations (see Table I). This is to be expected, since the rise time of the step was ~140 μs. Generally, we found that fibers having shorter extrapolated intercepts on the length axis were more difficult to obtain from the lumbricalis muscle than from the tibialis anterior, probably because of the greater relative contribution of tendon compliance in the shorter fibers.

Stiffness Measurement during Length Step Changes

To obtain stiffness measurements during the recovery of force after a step change in fiber length, length steps with

TABLE I

	Frequency	Stiffness	"y_0"	Tension	P/P_0
Tetanic plateau					
	(kHz)	*($\Delta P/P_0 \cdot \ell_0/\Delta\ell$)*	*(nm/half sarcomere)*	*($kN \cdot m^{-2}$)*	
Oscillations	1	177.0	6.2	296.6	1.0
	4	239.6	4.6	296.9	1.0
	7	252.9	4.3	294.9	1.0
	9	261.2	4.2	295.3	1.0
T_1 curve	—	211.3	5.2	292.0	1.0
Tetanic rise					
Oscillations	1	112.3	5.2	142.3	0.53
	4	165.1	3.5	155.9	0.53
	7	177.3	3.3	155.9	0.53
	9	186.8	2.8	139.0	0.47
T_1 curve	—	125.4	4.3	142.2	0.49

very small sinusoidal oscillations superimposed were performed on the tetanus plateau. Since the appearance of the sinusoidal length changes in the length step and force response signals made the peak to peak oscillation amplitude difficult to determine precisely, equal length steps were performed in the absence of sinusoidal length changes, and the records obtained were subtracted from those with sinusoidal length oscillations (e.g., Julian and Morgan, 1981). As a result, straight lines with superimposed sinusoidal oscillations were obtained for both force and length signals. Stiffness at various times during the force transient was plotted as a fraction of the stiffness measured immediately before the length step (Fig. 5). During the early part of the quick recovery, force was changing so rapidly that individual stiffness points could only be obtained for a single length oscillation at a time. It can be seen that the relative drop in force was much larger than the relative change in stiffness. For example, at the first stiffness point on the graph quick recovery had restored force to 54% of the value before the step and stiffness was 81% of its plateau value. Similar data were obtained from stretches, i.e., the change in stiffness resulting from a rapid stretch was always less than the change in force.

The value of "y_0" for this fiber was 5.17 nm per half sarcomere. We obtained the same result from the fiber of Table I, which had an intercept of 5.2 nm (i.e., following a quick release, stiffness was 80% of the plateau value when the force was 50% of the tetanic value). The mean value of the relative stiffness measured at 0.5 P_0 during the quick recovery was 80.1% (range 78 to 82%) of the value at P_0 in seven experiments.

The kind of experiment described above was repeated using a slower length step (1 ms), and stiffness was measured with sinusoidal length oscillations at 7 kHz. In this way, stiffness during a step release and during the quick recovery could be measured at a similar force level. Experimental records are shown in Fig. 6, and relative

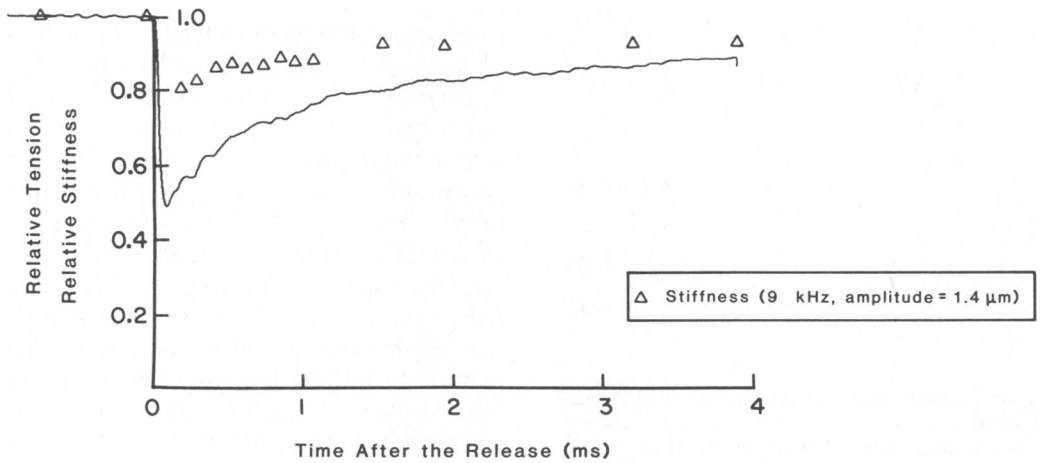

FIGURE 5 Stiffness after a quick release measured by sinusoidal oscillations. The relative stiffness (triangles) and relative tension (continuous line) during recovery from a step release of 4.5 nm per half sarcomere. Stiffness was calculated from superimposed sinusoidal length changes that were 1.4 μm in amplitude at 9 kHz, as described in the text. Both tension and stiffness are expressed relative to their values immediately before the step. This fiber was from the lumbricalis" digiti IV (1.vi.81), and was 2.28 mm long at a striation spacing of 2.2 μm and temperature of 4°C.

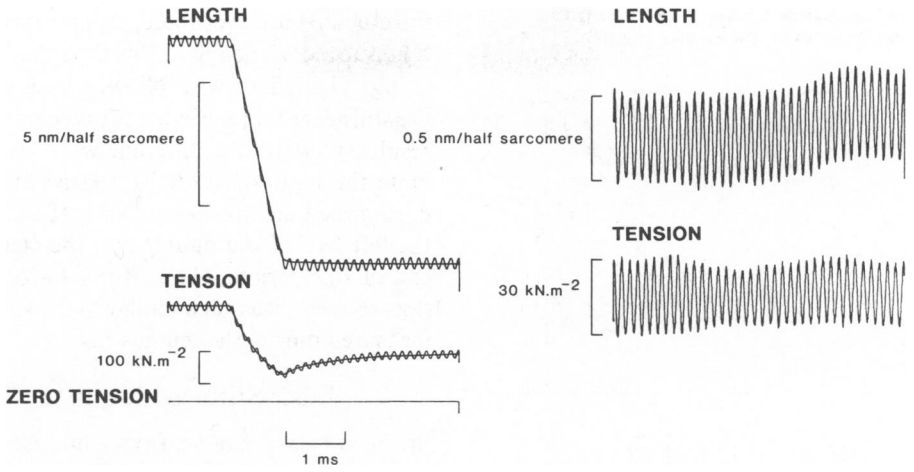

FIGURE 6 Stiffness measurements during a slow release and subsequent recovery. The records on the right of the figure were obtained by subtraction of the records with and without sinusoidal oscillations, shown on the left. Stiffness was calculated as described in the text. This fiber was from the lumbricalis" digiti IV (24.xii.81), and was 2.02 mm long at striating spacing 2.2 μm and temperature of 5°C. The oscillation frequency was 7 kHz and the amplitude was 1 μm.

stiffness and force during the release and subsequent recovery are shown in Fig. 7. In accordance with previous results (Ford et al., 1974), it can be seen that stiffness measured during the falling phase of force and during the rising phase of quick recovery are similar at a given relative force level.

Force-extension relationships were obtained for a step release and subsequent restretch applied during the quick recovery, using length steps adjusted to have a constant velocity during the period we measured to avoid distortions from the inertia of the fiber. A linear regression was then performed on points obtained over an identical force range during the release and subsequent restretch to detect differences in fiber stiffness. The data obtained were compared at different times during the quick recovery. This comparison is shown in Fig. 8. When we used this method, stiffness measurements during the quick recovery were also very similar to those obtained during the initial release. Hence, these results as well as those using slower length steps and high frequency sinusoids of length to measure stiffness directly suggest that stiffness remained almost constant during the quick recovery.

Fig. 9 shows the results from an experiment in which the time course of the stiffness and force changes were measured over a period of 200 ms during the recovery after a relatively big step release (1% of fiber length). The step applied was bigger than the amount necessary to send the force to zero (0.8% of fiber length). The first measurement of the stiffness was made when the force had recovered to 0.12 P_0. At this level of force, the relative stiffness was 0.5. Also shown are the stiffness and force measured during the tetanus rise. Within the first 10 ms after the big release and

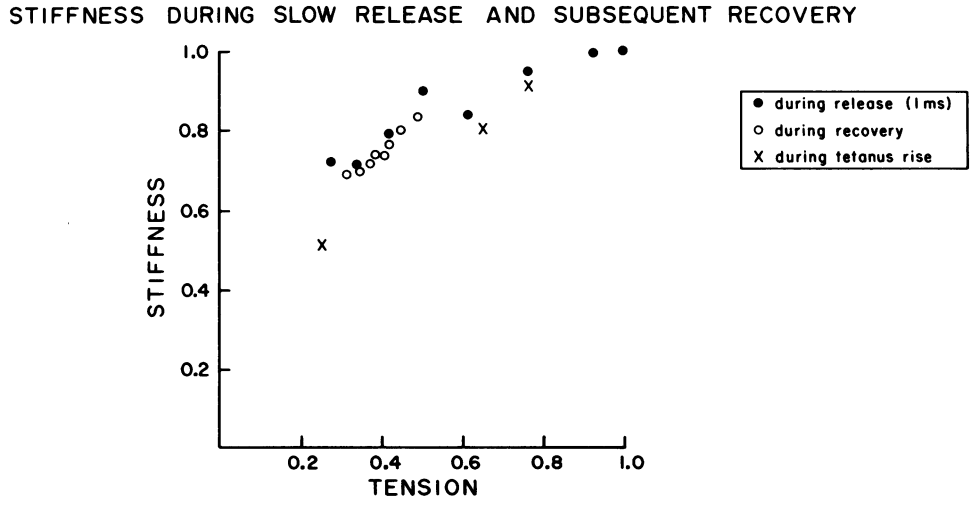

FIGURE 7 Relative stiffness and relative tension during a slow release (●), and the subsequent recovery (○) obtained from the data in Fig. 6. The relation between stiffness and tension during the rise of a tetanus from the same fiber is also shown (X).

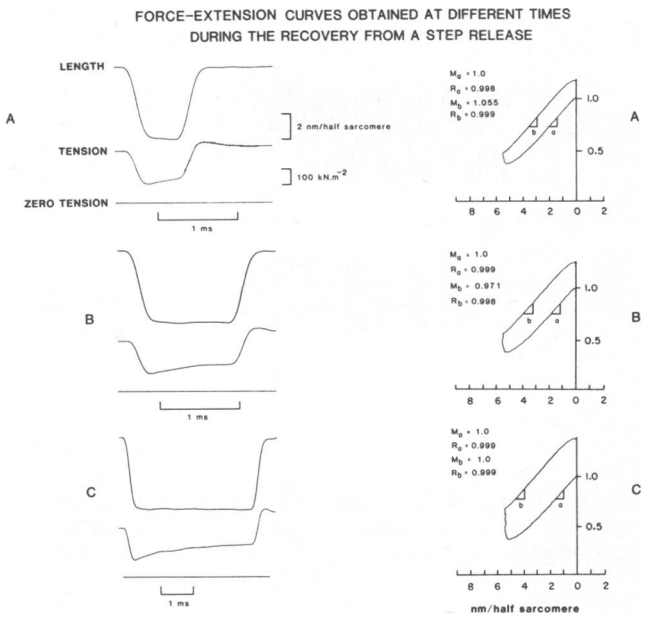

FIGURE 8 Force-extension curves determined at three different times during the recovery from a quick release. The column of traces on the left show the length and force responses to a release during the tetanic plateau followed by a restretch at a progressively later time during recovery. Note that the time scale for the records in *C* is compressed compared to *A* and *B*. The right-hand column shows a force-extension plot for each corresponding set of records, which is a measure of the degree of association between these two variables. Tension relative to the pre-release tetanic value (i.e., 1.0) is each ordinate, and length change in nanometers per half sarcomere is each abscissa. A right triangle (lowercase *a* and *b*) was drawn on the part of each force-extension plot that coincided with the middle of the length step. The slope of the hypotenuse of each triangle was compared with the other of each pair (i.e., *a* to *b*) by linear regression analysis. The rate of change at the different times gives an estimate of stiffness during a release (M_a) relative to stiffness during a restretch (M_b), and the correlation coefficients (R_a and R_b) describe the degree to which the data predict a perfect positive correlation (i.e., $R = +1.000$) between the variables. This fiber is the same one used for in Figs. 6 and 7.

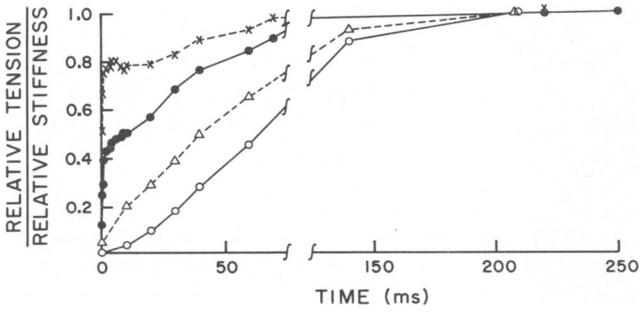

FIGURE 9 The time course of stiffness and tension changes during the tetanus rise (Δ, stiffness; O, tension) and during the recovery from a relatively big (1% of ℓ_o) release (X, stiffness; ●, tension). This fiber was from the lumbricalis" digiti IV (10.xi.81), and was 2.3 mm long at striation spacing 2.25 μm and temperature at 4°C. The frequency of oscillation was 4 kHz and the oscillation amplitude was 1.2 μm peak to peak.

the quick recovery of force, a slight fall in stiffness (Fig. 9, X) occurred, although at this time the force (Fig. 9, ●) was rising. This phase was followed by a gradual recovery of the stiffness that preceeded the recovery of force. The same results, plotted in a different way, are shown in Fig. 10. Note the high value of the relative stiffness (Fig. 10, X) during the quick recovery phase after the big release (i.e., the left half of the figure) and the change in slope at the end of this period. The stiffness-to-force ratio during the slow recovery was very similar to the stiffness-to-force ratio measured during the tetanus rise.

Fiber Stiffness during the Tetanus Rise

Stiffness measurements from sinusoidal length oscillations were obtained at various times during the tetanus rise using frequencies in the range 1 to 9 kHz. The experimental records obtained for a short fiber by this procedure are shown in Fig. 4. The calculated stiffness values are reported in Table I. The stiffness-to-force ratio during the tetanus rise was not constant, in contrast to the results observed by others (Huxley and Simmons, 1972; Julian and Sollins, 1975). The mean relative stiffness obtained at 4 kHz from four experiments of this type at a mean force of 0.5 P_0 during the tetanus rise, was 0.67 (range 0.66 to 0.69) of the tetanic value. The deviation from a constant stiffness to force relationship can be accounted for by a lead of stiffness changes over force of ~15 ms (see Fig. 9). This lead was more pronounced at high frequencies (e.g., 9 kHz) than at low frequencies (e.g., 1 kHz). The effect of such a lead of stiffness over force should reduce the value of the extrapolated intercept at zero force obtained from the T_1 curve during the tetanus rise. It can indeed be seen from Table I that the extrapolated intercept of the T_1 curve obtained on the tetanus rise at a force of 0.5 P_0 was considerably reduced; it had a value of 4.3 nm per half sarcomere compared with the value of 5.2 nm obtained on the tetanus plateau. Furthermore, at low force levels in the frequency range 1 to 4 kHz we observed a greater phase lead of force over length compared with the plateau.

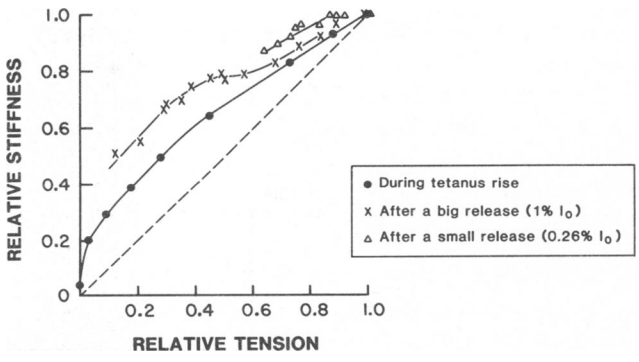

FIGURE 10 The correlation between relative stiffness and relative tension replotted from the data of Fig. 9. The relative stiffness obtained during recovery from a small (0.26% ℓ_o) quick release is also shown (Δ). The dashed line indicates a constant ratio between stiffness and tension.

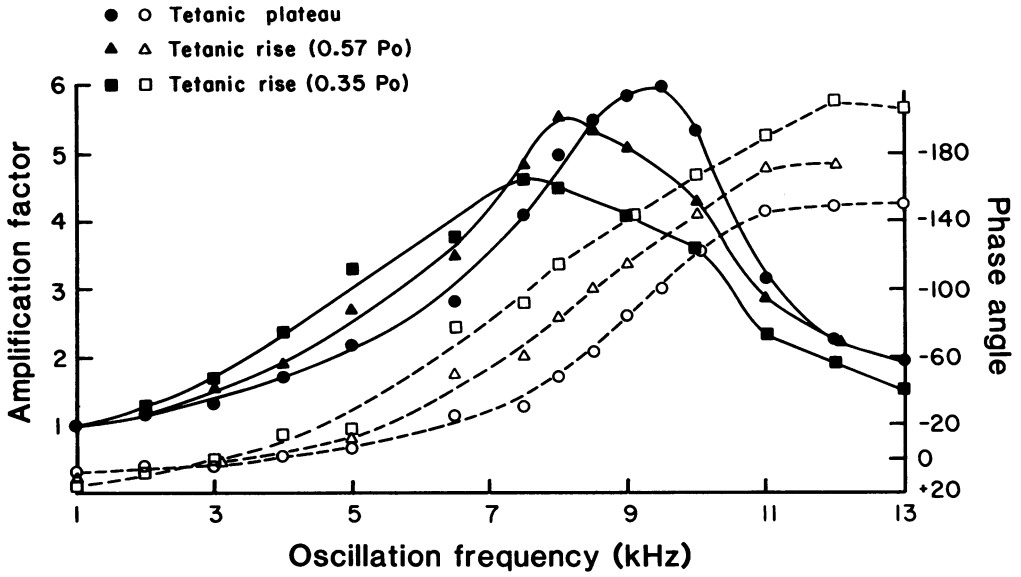

FIGURE 11 Frequency dependence of force responses to small amplitude sinusoidal length changes. Filled symbols, amplitude of force oscillations relative to the amplitude at 1 kHz; open symbols, phase angle between length and force. Squares and triangles, experimental points obtained during the tetanic rise at 0.35 and 0.57 P_o, respectively. Circles, experimental points at the plateau. Note the small phase lead of the force over length at 1 kHz. This is the same fiber as in Fig. 2.

The stiffness of a stimulated fiber can also be obtained from the experimental measure of the resonance frequency of the fiber and this procedure can be used during the tetanic plateau and during the tetanus rise. With this type of experiment, it was possible to use long fibers, which reduced the contribution of the tendon compliance to the overall compliance of the preparation. A typical result is reported in Fig. 11. A series of sinusoidal length changes at different frequencies were applied to the fiber during the tetanic plateau and during the tetanus rise, when the force was 0.35 and 0.57 P_0. The relative force output and phase shift are plotted as a function of frequency. It can be seen that the resonance frequency is force-dependent, being 9.30 kHz during the tetanic plateau and 8.25 and 7.25 kHz at 0.57 and 0.35 P_0, respectively. The mean relative stiffness obtained from three experiments of this type at a mean force of 0.55 P_0 was 0.72. This value agrees with the value of 0.67 obtained at 0.5 P_0 by measuring the stiffness as the ratio of force to length oscillations in short fibers, confirming that during the tetanus rise the relative stiffness is higher than the relative force. Note that during the tetanus rise the mechanical amplification is reduced compared to the plateau value. This could be due to more effective damping at lower stiffness.

The fact that the relative stiffness is higher than the relative force during the tetanus rise could be explained by the presence of an external compliance (e.g., tendons) with appropriate characteristics. To test this possibility, we measured the stiffness directly (i.e., $\Delta P/\Delta \ell$ during the steady state for active tension in a series of contractions of various amplitudes) and compared the values to the stiffness-to-force ratio obtained under normal conditions during the tetanus rise. Tetrodotoxin (TTX) was added to the bathing solution to block regenerative electrical responses. Then the fibers were returned to normal Ringer and fused, sustained contractions of different amplitudes were obtained at 5-min intervals using AC field stimulation (50 Hz) as the fibers recovered from the TTX. Force recovers slowly when TTX is removed, perhaps because TTX might diffuse slowly in the transverse tubular system (Bastian and Nakajma, 1974). When regenerative electrical responses are blocked in this way, the membrane potential

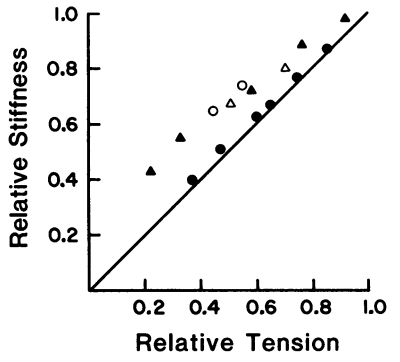

FIGURE 12 Relative stiffness and relative tension measured at the plateau of contractions of various amplitudes. TTX was added to the bath (final concentration 10^{-6} M) to block the circumferential and radial spread of depolarization produced by an increase in sodium conductance. The fiber (30.x.81) was activated by sinusoidal AC field stimulation (50 Hz). The stiffness was measured at the plateau (●) and during the rise of tension (○). The open triangles are control points obtained with brief, square DC-field stimulation after a complete recovery in normal Ringer. The filled triangles were obtained during the rise of tension before the addition of TTX. This fiber was from the tibialis anterior, was 6.9 mm long at striation spacing 2.2 μm and temperature of 4°C. The frequency of oscillation was 2.5 kHz.

is presumably graded with the field strength of a transversely applied alternating current (Mashima and Washio, 1968; Bromm and Simon, 1971). A typical result from this type of experiment is shown in Fig. 12. The normalized stiffness-to-force relationship of the points obtained during the steady state of AC field-induced contractions (i.e., Fig. 12, ●), which are graded in amplitude, fall very close to the straight line. Only under these conditions, in which the membrane potential was presumably no more than partially depolarized (Sten-Knudsen, 1957) and the sodium-dependent radial spread of contraction was impaired (Bastian and Nakajima, 1974), did our results indicate a direct proportionality between stiffness and force. This result was found consistently in four experiments of this type. On the other hand, note that the points obtained with AC field stimulation during the *rise* of force (i.e., Fig. 12, ○) fall very close to the points obtained during the tetanus rise in normal conditions. We have previously considered the possibility that compliance from various sources might influence our results (Cecchi et al., 1982*c*). This result (Fig. 12) is additional evidence against the possibility that an internal compliance could cause the stiffness-to-force ratio obtained during the tetanus rise to become inconstant.

DISCUSSION

Fiber Resonance

The mechanical behavior of a single muscle fiber can be better described by a distributed rather than a lumped model (Schoenberg et al., 1974; Ford et al., 1981). The simplest distributed model would be one involving only inertia and compliance, as proposed by Schoenberg et al. (1974). To account for the form of the curves in Figs. 2 and 11, a viscous component must be added to their model. Such a system will show mechanical amplification of sinusoids of force and a phase lag of force compared to length as the frequency of the length oscillations approach the resonance frequency of the muscle. The general features of Fig. 2 can be reproduced from a transmission line consisting of elasticity, viscosity, and mass, as described by Ford et al. (1981), and our Fig. 2 may be generally useful in predicting approximately the amount of force amplification that will occur at different driving frequencies, as long as the wavelength of the oscillations is large compared with the cross-sectional area of the muscle preparation.

During direct measurements of fiber stiffness in the range 1 to 9 kHz, we saw no indication of resonance, i.e., no change in the phase angle records, when we used short fibers from the lumbricalis muscle. At low frequencies (1 to 4 kHz), the stiffness of the preparation usually increased by a factor of ~1.3 from 1 to 4 kHz, and at 1 kHz a phase lead of force relative to length changes was present. These observations are consistent with the possibility that the reduced amplitude of force at 1 kHz was caused by a rapid early recovery response to reduction of length. This effect is similar to that causing truncation in stiffness measurements made from step length changes (Ford et al., 1977). Beyond 4 kHz, this recovery apparently becomes less important, and a change in stiffness by a factor of ~1.1 was observed in the range 4 to 9 kHz. From Table I it can be seen that the value of "y_0" obtained on the tetanus plateau using 9 kHz oscillations was 4.2 nm per half sarcomere, which is similar to the value proposed by Ford et al. (1977) in the absence of truncation.

Stiffness on the Tetanus Rise

During the tetanus rise, we measured a higher relative stiffness compared with that at the plateau. When two oscillation frequencies were used, the higher frequency yielded higher relative stiffness measurements. In addition, at 4 kHz, a frequency at which no phase shift was present during the tetanus plateau in short fibers (e.g., Fig. 1), a small phase lead of force over length was measured during the tetanus rise. These observations are consistent with the possibility that there is a faster rate of recovery on the rise compared with the plateau. The relatively high stiffness measured during the tetanus rise can be accounted for in at least four ways. First, fiber resonance might have caused the data we report here on fiber stiffness to be overestimated during the tetanus rise. Second, there might be a reduction in the degree of truncation of force during the tetanus rise, leading to a higher relative stiffness at low forces. Third, there might be an effect from a series elastic element that could affect the data by causing erroneous estimates of cross-bridge stiffness, or this putative elastic element might permit significant shortening of the fiber during the tetanus rise that would allow attached cross-bridge states to range between isometric and isotonic distributions. Finally, there may be a significant population of attached, nonforce generating cross-bridges during the tetanus rise. In the following paragraphs, we consider these individual possibilities.

As can be seen in Eq. 3 and Fig. 2, a reduction in Young's modulus could cause an increase in mechanical amplification at a given frequency as a result of a reduction in the resonance frequency of the fiber. The question then becomes whether the resonance frequency of the fiber could become low enough to account for the unexpectedly high stiffness during the tetanus rise? According to Eq. 3, if stiffness were proportional to force throughout the tetanus rise, then at 0.50 P_0 we should expect to have a value for Young's modulus that is 50% of that obtained at the plateau. Given these values, a resonance frequency of 38 kHz for the fiber, an oscillation frequency of 4 kHz, and an absence of damping, one would expect a mechanical amplification of ~2% on the plateau, and ~4% at 0.50 P_0. Such an amplification could not account for our data. In fact, an amplification of ~40% would be required. Furthermore, it can be seen from Table I that the relative stiffness measured during the rise at 4 kHz is almost equal to the

stiffness measured at 7 kHz, again indicating no significant effect from the resonance.

The second possibility, that the recovery mechanisms are slower during the tetanus rise, seems equally unlikely. As a rule, measurements of fiber stiffness during the tetanus rise with low oscillation frequencies (1 to 3 kHz) showed that force oscillations lead length changes during the tetanus rise at low force levels, which suggests that the tension recovery mechanism might be even faster during the tetanus rise than during the plateau. In addition, the resonance frequency of a fiber measured on the tetanus rise by applying different frequencies of sinusoidal length changes (Fig. 3) indicated that the stiffness was again higher than expected from a constant stiffness-to-force ratio. The frequencies used (6–10 kHz) were high enough to avoid a large part of the tension recovery and should indicate the true stiffness of the fiber.

The presence of an additional series compliance in the preparation could permit shortening of the fiber during the tetanus rise at the expense of this unknown compliance. According to A. F. Huxley (1957), such shortening would result in a higher stiffness-to-force ratio than that obtained under truly isometric conditions. Accordingly, if shortening were the cause of the high stiffness-to-force ratios reported here on the tetanus rise, it should be possible to calculate the velocity of shortening required. Such a calculation indicates that the amount of extra series elasticity required would not be consistent with the form of the T_1 curve obtained (Cecchi et al., 1982*c*).

Alternatively, the additional series elastic element could affect stiffness measurements directly. For example, an exponential series compliance would yield a constant stiffness-to-force ratio, whereas a Hookean stiffness would give a gradually increasing stiffness to force ratio as force is decreased. Our data could be accounted for by the presence of an additional series elastic element with Hookean characteristics. But this element would have to have a compliance accounting for ~50% of the total fiber stiffness. Since the measurements of Ford et al. (1981) indicate that possible sources of sarcomere compliance other than that associated with the cross-bridges can account for only ~10% of the total compliance per half sarcomere, the additional compliance must be extracellular. Such additional extracellular compliance would then have produced a large deviation of the values for the extrapolated intercept of our T_1 curves from those values reported by Ford et al. (1977). The T_1 curve obtained for the fiber in Table I, for example, agrees rather well with the points obtained by Ford et al. (1977), whose values were obtained using a spot follower device to compensate for tendon compliance. Further evidence against this possibility is the result shown in Fig. 12. The correlation between stiffness and force obtained in contractions graded in amplitude is linear, whereas the same relationship in the same fiber is not linear when stiffness and force are measured during the tetanus rise. In addition, the contribution of tendon compliance to total stiffness is lower in a long fiber, such as that used for Fig. 11. Nevertheless, the observed shift in the resonance frequency in this fiber was still consistent with a higher relative stiffness on the tetanus rise than at the plateau. Finally, a compelling point to support this idea is that the same result has recently been reported in experiments with a striation follower, where the effects of extracellular compliance are eliminated (Cecchi et al., 1984). We conclude it is unlikely that an additional series elastic element could account for our data.

The final explanation that we are left with is the possibility that attached cross-bridges initially pass through a state in which they contribute to stiffness, but not to force development. In essence, an attached nonforce generating cross-bridge state has been proposed by Huxley and Simmons (1971). However, the state we propose would differ from those described by Huxley and Simmons (1971) to account for the quick recovery after a step length change, since transitions between their states occur with rate constants of the order of hundreds of reciprocal seconds. The change of the attached state on the tetanus rise that we propose would be much slower. Our data lead us to suggest that the lag of tension with respect to stiffness is consistent with a rate constant for tension development by attached cross-bridges that is an order of magnitude lower than the rate constant governing the quick recovery. This is clearly evident in Fig. 9.

Such a delay between attachment and force production of cross-bridges during the twitch or tetanus rise has been suggested by H. E. Huxley (1976) and Matsubara and Yagi (1978) as a possible explanation for x-ray diffraction data showing that movement of the cross-bridge heads towards actin filaments leads force development by some 15 ms. In addition, it has been reported that during the stretch activation of glycerinated insect flight muscle a rise in stiffness precedes force (Herzig, 1977), although this result is disputed (White et al., 1977). The idea that cross-bridge attachment noticeably precedes force development has now been supported by data obtained from several techniques, and is unlikely to be an unexplained anomaly of a given approach (Mason and Hasan, 1980; Tamura et al., 1982; Schoenberg and Wells, 1984).

Fiber Stiffness after a Step Length Change

According to the model of Huxley and Simmons (1971), the recovery of force following a step change in fiber length occurs as a result of the rotation of attached cross-bridges, and does not involve a net attachment or detachment of these bridges. The stiffness of the cross-bridge in their model is believed to be Hookean, which means that the instantaneous stiffness of the fiber before the step should be the same as that during the quick recovery. Ford et al. (1974) found a reduction of fiber stiffness of ~4% during the quick recovery, as measured from force extension curves obtained during the initial release and a subsequent

restretch applied during the quick recovery phase. Since Ford et al. (1974) made their measurements at comparable force levels, the compliance of the tendons was effectively cancelled, and so they attributed the reduction in stiffness during the recovery from the release to an enhanced detachment rate. The data presented in this paper indicate a much larger fall in *total* stiffness as a result of the rapid release. The mean decrease in stiffness at 0.5 P_0 (measured with 4-kHz oscillation) was 19.9% (range 18–22%) in seven fibers. This observation is not necessarily at odds with the data of Ford et al. (1974), since our data were measured at a different force level at the plateau and during the recovery. Consequently, our results could be altered by a non-Hookean stiffness associated with the tendons. As can be seen in Fig. 5, stiffness and force do not recover at the same rate immediately after a quick release. However, the stiffness measured by sinusoidal oscillations at a given force level during a slower release (Fig. 6) was only slightly different from the stiffness measured at the same force level during the quick recovery. This was confirmed by measuring the slope of force-extension curves obtained during the initial release and during the quick recovery. From these latter two kinds of experiment, we estimated that the change in fiber stiffness during the quick recovery was <4%, i.e., the quick recovery occurred without significant detachment of cross-bridges.

During our experiments to determine the complete time course of changes in fiber stiffness, a small fall in stiffness was detected at the end of the quick recovery (phase 3 of Ford et al., 1977) from a quick release at a time ~10 ms after the end of the step. This could not be satisfactorily accounted for by tendon compliance, since it occurred while force was increasing (Fig. 9), and this change may indeed indicate a net detachment of cross-bridges. After this reduction, the ratio of recovery of force and stiffness was similar to that observed on the tetanus rise with the recovery of stiffness preceding the recovery of force.

APPENDIX

An Estimate of Recorded Force Amplitudes and Phase Angles Between Force and Applied Sinusoidal Length Changes

An isolated muscle fiber may be regarded as a uniform rod, comprised of longitudinally distributed elements of mass, compliance, and viscosity. A longitudinal wave transmitted along the rod encounters forces from these elements in addition to a force component from the viscosity of the surrounding medium. The transmission of such a longitudinal wave can be described by modifying the familiar wave equation to the following form:

$$E\frac{\partial^2 u}{\partial x^2} + \mu\frac{\partial^3 u}{\partial x^2 \partial t} = \rho_f\frac{\partial^2 u}{\partial t^2} + \sigma\frac{\partial u}{\partial t}, \tag{A1}$$

where E is Young's modulus, μ is the internal damping coefficient, ρ_f is the density of the fiber, and σ is the external damping coefficient. The displacement at position x and time t is represented by $u(x, t)$.

One may assume a general solution for this kind of equation of the following type:

$$u(x, t) = Ae^{2\pi if(t+x/c)e^{\gamma x}} + Be^{2\pi if(t-x/c)e^{-\gamma x}}. \tag{A2}$$

This equation applies after initial transient states have died away, when A and B are arbitrary constants determined from the boundary conditions of the problem, and c and γ are parameters describing the velocity and damping of the transmitted wave. If we substitute Eq. A2 in Eq. A1, equate the real and imaginary parts of the resulting equation, and make the substitution $\gamma = 2\pi\alpha/c$, we obtain expressions for c and α for the following form:

$$c^2 = \frac{E}{\rho_f}\left(1 - \frac{\alpha^2}{f^2}\right) + \frac{4\pi\mu\alpha}{\rho_f} \tag{A3}$$

$$\alpha^2\left(1 + \frac{\sigma E}{4\pi^2 f^2 \mu\rho_f}\right) + \alpha\left(\frac{E}{\pi\mu} - \frac{\sigma}{\pi\rho_f}\right) - f^2 - \frac{\sigma E}{4\pi^2\mu\rho_f} = 0. \tag{A4}$$

The positive root of α allows one to directly evaluate c from this.

Where U_{max} is the peak value of $u(L, t)$ the boundary conditions of Eq. A1 are taken to be

$$u(L, t) = U_{max}e^{2\pi ift} \tag{A5}$$

$$u(0, t) = 0. \tag{A6}$$

Hence $B = -A$, and

$$u(L, t) = Ae^{2\pi ift}\,(e^{2\pi ifL/c}\,e^{\gamma L} - e^{-2\pi ifL/c}\,e^{-\gamma L}) \tag{A7}$$

$$U_{max} = 2A\left(\sin h[\gamma L]\cos\left[\frac{2\pi fL}{c}\right] + i\cos h[\gamma L]\sin\left[\frac{2\pi fL}{c}\right]\right). \tag{A8}$$

Thus, the force at the transducer, including viscous effects, is

$$F(o, t) = E\frac{\partial u}{\partial x} + \mu\frac{\partial^2 u}{\partial x\partial t} = (E + 2\pi i\mu f)\left(\gamma + \frac{i2\pi f}{c}\right)2Ae^{2\pi ift}. \tag{A9}$$

Hence, $M(f)$, the ratio of the force response as a function of frequency at $x = 0$ to a sinusoidal length oscillation driven to an amplitude of U_{max} when $x = L$, is

$$M(f) = \frac{F_{max}\,(x = o)}{U_{max}\,(x = l)} = \frac{(E + i2\pi\mu f)(\alpha + if)\frac{2\pi}{c}}{\sin h\left(\frac{2\pi\alpha L}{c}\right)\cos\left(\frac{2\pi fL}{c}\right) + i\cos h\left(\frac{2\pi\alpha L}{c}\right)\sin\left(\frac{2\pi fL}{c}\right)}. \tag{A10}$$

By substitution of $\gamma = 2\pi\alpha/c$, this has a magnitude of

$$|M(f)| = \frac{\frac{2\pi L}{c}[(E^2 + 4\pi^2\mu^2 f^2)(\alpha^2 + f^2)]^{1/2}}{E\left[\sin h^2\left(\frac{2\pi\alpha L}{c}\right)\cos^2\left(\frac{2\pi fL}{c}\right) + \cos h^2\left(\frac{2\pi\alpha L}{c}\right)\sin^2\left(\frac{2\pi fL}{c}\right)\right]^{1/2}}, \tag{A11}$$

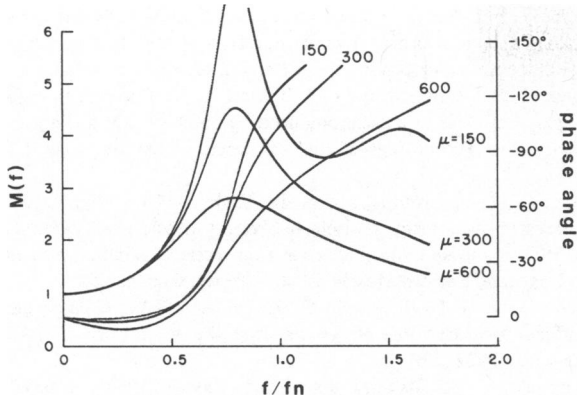

FIGURE 13 The relation between force amplitude, phase angle, and frequency of applied sinusoidal length change based on the equations, corrections, and assumptions in the appendix. Force amplification, $M(f)$, is plotted on the left-hand ordinate; phase angle, in degrees, is on the right-hand ordinate. Frequency (f/f_n) on the abscissa varies from 0 to 2. The curves of force amplitude and phase angles here vary from smallest to largest as the internal damping coefficient (μ) varies from 600 to 300 to 150 N · s · m^{-2}. Compare with Fig. 2.

with a phase shift of

$$\phi + \delta - \theta, \tag{A12}$$

where

$$\tan\theta = \cot h\left(\frac{2\pi\alpha L}{c}\right)\tan\left(\frac{2\pi fL}{c}\right) \tag{A13}$$

and

$$\tan\delta = \frac{2\pi\mu f}{E} \tag{A14}$$

and

$$\tan\theta = f/\alpha. \tag{A15}$$

The values of the fiber density and external damping are probably not true constants but vary as a function of frequency, as described by Ford et al. (1977). In this case, they can be corrected at a sarcomere length of 2.1 μm, as Ford et al. (1977) suggest, by use of the following relationships:

$$\omega = \frac{P}{(\pi ab)^{1/2}},\ \gamma = \left(\frac{\eta}{\pi\rho_m f}\right)^{1/2} \tag{A16}$$

$$\rho' f = \rho f + \frac{\omega\rho_m\gamma}{2}\left(\frac{1}{\pi ab}\right)^{1/2} \tag{A17}$$

$$\sigma = \left(\frac{2\pi\eta f\rho_m(a^2+b^2)}{a^2b^2}\right)^{1/2}, \tag{A18}$$

where $2a$ and $2b$ represent the maximum and minimum diameters of a fiber respectively, P is the circumference of a fiber (assumed to be elliptical and, therefore, approximately equal to $2\pi[0.5(a^2+b^2)]^{1/2}$), η is the viscosity of the medium, ρf is the true fiber density, $\rho' f$ is the corrected fiber density and ρ_m is the density of the surrounding fluid.

By applying these corrections and assuming (a) a value for Young's modulus of 6.25 × 10^7 N · m^{-2}, (b) viscosity of water 1.8 × 10^{-3} N · s · m^{-2}, (c) density of Ringer solution 10^3 kg · m^{-3}, (d) density of fiber 1.037 × 10^3 kg · m^{-3}, (e) major fiber diameter 148 μm, (f) minor fiber diameter 91 μm, (g) fiber length 11 mm, we obtained the theoretical curves shown in Fig. 13. One can compare the values we measured with the responses predicted by this model by reference to Figs. 2 and 11 of the text. The solution for three different values of the internal damping coefficient are shown in Fig. 13 (150, 300, and 600 N · s · m^{-2}). One can see that the amplitude of the force response is extremely dependent on the value of μ that is chosen. However, the position of $M(f)$ at its maximum is influenced very little by μ. The value corresponding to that of Ford et al. (1977) in resting fibers would be 300 N · s · m^{-2}, which would give a reasonably good fit to the experimental data in Fig. 2 of the text. However, since the quick recovery of tension that follows a length change would tend to cause an underestimate of the force response at low frequencies, the actual peak force amplitude as a function of frequency

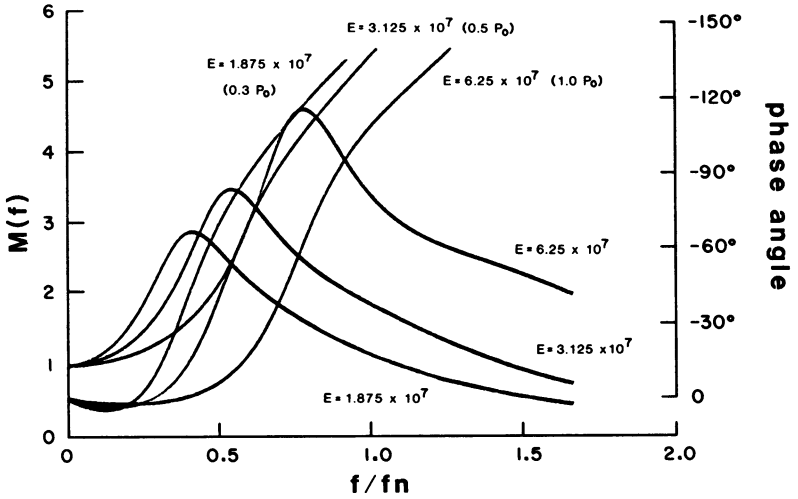

FIGURE 14 Relationships to maximum active tension (P_o). The curves of force amplitude and phase angles in Fig. 13 were all calculated with the same internal damping coefficient (μ = 300 N · s · m^{-2}). The value for Young's modulus was 1.875, 3.125, and 6.25 × 10^7 N · m^{-2} for each curve from left to right, respectively. σ = 9.08 × 10^6 N · s · m^{-2} = external damping coefficient; ρ_f = 1.037 × 10^3 kg · m^{-3} = fiber density; L_{tot} = 11 mm; S = 2.1 μm. The peaks shift from left to right as tetanic tension changes from 0.3 to 0.5 to 1.0 times the maximum during the tetanus plateau. Compare with Fig. 11.

may be reduced by ~30%. We suggest that the likely value of μ is on the order of 300 to 350 $N \cdot s \cdot m^{-2}$ during the tetanus plateau in these fibers.

The model also predicts relatively little effect of internal or external damping on the position of the maximum value of $M(f)$, which should, therefore, be principally dependent on the value of Young's modulus. Hence, it is unlikely that the change in position of the peak of $M(f)$ during the tetanus rise (text Fig. 11) is strongly influenced by changes in fiber viscosity. The model (Fig. 14) is not similar enough to Fig. 11 to support the idea that stiffness and force have a constant relationship. The movement of the peak of $M(f)$ in text Fig. 11 can perhaps be used as a measure of a change in stiffness.

A group of waves such as those transmitted after a sharp step will propagate at a group velocity of

$$V_g = c + f\frac{dc}{df} \tag{A19}$$

if

$$\frac{\sigma}{\pi\rho_f} \ll \frac{E}{\pi\mu} \text{ and } \alpha^2 \ll f^2, \text{ then } f\frac{dc}{df} \simeq \frac{4\rho\mu\alpha}{\rho_f c}. \tag{A20}$$

This suggests that high frequency components that follow a very rapid step would propagate faster than low frequency components. For example, for the fiber of Fig. 2, components at 40 kHz would propagate almost four times faster than components at 4 kHz. This would account for the difference between our measured step transmission time and the transmission time calculated from the fiber resonance curve, and would also account for the phase shift observed at the start of sinusoidal oscillations compared with that at the steady state.

We have assumed, for purposes of this appendix, that the internal damping coefficient should be a true viscous component. However, we cannot discount the possibility that this apparent viscosity might represent some mechanochemical process occurring with a very fast rate constant in a muscle fiber.

We are indebted to L. A. Wanek for preparing the fibers gripped by clasps and to L. F. Wussow for preparing the figures and the manuscript. Appendix prepared with the assistance of J. M. Baker, Clarendon Laboratory of Physics, Oxford, OX1 3PT, England.

Supported by the Muscular Dystrophy Association, the Minnesota Heart Association, and the U.S. Public Health Service (NS 14268).

Received for publication 27 March 1984 and in final form 11 September 1985.

REFERENCES

Bastian, J., and S. Nakajima. 1974. Action potential in the transverse tubules and its role in the activation of skeletal muscle. *J. Gen. Physiol.* 63:257–278.

Blangé, T., J. M. Karremaker, and A. E. J. L. Kramer. 1972. Tension transients after quick release in rat and frog skeletal muscle. *Nature (Lond.).* 237:281–283.

Bressler, B. H., and N. F. Clinch. 1974. The compliance of contracting skeletal muscle. *J. Physiol. (Lond.).* 237:477–493.

Bromm, B., and R. Simon. 1971. Inward rectification in frog skeletal muscle during alternating current stimulation. *Pfluegers Arch. Eur. J. Physiol.* 328:365–378.

Cambridge, G. W., and J. Haines. 1959. A new versatile transducer system. *J. Physiol. (Lond.).* 149:2–3P.

Cecchi, G. 1983. A circuit specially suited for use with high-frequency capacitance gauge force transducers. *Arch. Ital. Biol.* 121:215–217.

Cecchi, G., F. Colomo, and V. Lombardi. 1976. A loudspeaker servo system for determination of mechanical characteristics of isolated muscle fibres. *Boll. Soc. Ital. Biol. Sper.* LII:733–736.

Cecchi, G., F. Colomo, V. Lombardi, and G. Piazzesi. 1984. Stiffness and isometric tension during tetanus rise in frog muscle fibre segments under length-clamp conditions. *J. Physiol. (Lond.).* 357:104P.

Cecchi, G., P. J. Griffiths, and S. R. Taylor. 1981*a*. Decrease in aequorin response of skeletal muscle produced by quick release during tetanic contraction. Proceedings of the VII International Biophysical Congress. 177.

Cecchi, G., P. J. Griffiths, and S. R. Taylor. 1981*b*. High frequency stiffness measurements on isolated skeletal muscle fibers. Abstract of ASPET Symposium on Excitation-Contraction Coupling in Skeletal, Cardiac, and Smooth Muscle. Banff, Alberta, Canada. 26.

Cecchi, G., P. J. Griffiths, and S. R. Taylor. 1982*a*. High frequency stiffness measurements of isolated frog skeletal muscle. *J. Physiol. (Lond.).* 324:22–23P.

Cecchi, G., P. J. Griffiths, and S. R. Taylor. 1982*b*. Mechanical resonance of single muscle fibers studied by high frequency sinusoidal vibrations. *Biophys. J.* 37 (2, Pt.2):120*a*. (Abstr.).

Cecchi, G., P. J. Griffiths, and S. R. Taylor. 1982*c*. Muscular contraction: kinetics of crossbridge attachment studied by high frequency stiffness measurements. *Science (Wash. DC).* 217:70–72.

Ford, L. E., A. F. Huxley, and R. M. Simmons. 1974. Mechanism of early tension recovery after a quick release in tetanized muscle fibres. *J. Physiol. (Lond.).* 240:42–43P.

Ford, L. E., A. F. Huxley, and R. M. Simmons. 1977. Tension responses to sudden length change in stimulated frog muscle fibres near slack length. *J. Physiol. (Lond.).* 269:441–515.

Ford, L. E., A. F. Huxley, and R. M. Simmons. 1981. The relation between stiffness and filament overlap in stimulated frog muscle fibres. *J. Physiol. (Lond.).* 311:219–249.

Griffiths, P. J., H. J. Kuhn, K. Güth, and J. C. Rüegg. 1979. Rate of isometric tension development in relation to calcium binding of skinned muscle fibres. *Pfluegers Arch. Eur. J. Physiol.* 382:165–170.

Herzig, J. W. 1977. A model of stretch activation based on stiffness measurements on glycerol extracted insect fibrillar flight muscle. *In* Insect Flight Muscle. R. T. Tregear, editor. North Holland Publishing Company, Amsterdam. 209–219.

Huxley, A. F. 1957. Muscle structure and theories of contraction. *Prog. Biophys. Biophys. Chem.* 7:255–318.

Huxley, A. F., R. M. Simmons. 1971. Proposed mechanism of force generation in striated muscle. *Nature (Lond.).* 213:533–538.

Huxley, A. F., and R. M. Simmons. 1972. Mechanical transients and the origin of muscular force. *Cold Spring Harbor Symp. Quant. Biol.* 37:669–680.

Huxley, A. F., and V. Lombardi. 1980. A sensitive force transducer with a resonant frequency of 50 kHz. *J. Physiol. (Lond.).* 305:15P.

Huxley, H. E. 1976. Introductory remarks: the relevance of studies on muscle to problems of cell motility. *Cold Spring Harbor Conf. Cell Proliferation.* 3:115–126.

Julian, F. J., and M. R. Sollins. 1975. Variation of muscle stiffness with force at increasing speeds of shortening. *J. Gen. Physiol.* 66:287–302.

Julian, F. J., and D. L. Morgan. 1981. Variation of muscle stiffness with tension during tension transients and constant velocity shortening in the frog. *J. Physiol. (Lond.).* 319:193–203.

Kawai, M. 1982. Correlation between exponential processes and crossbridge kinetics. *In* Basic Biology of Muscles: A Comparative Approach. B. M. Twarog, R. J. C. Levine, and M. M. Dewey, editors. Raven Press, New York. 109–130.

Kawai, M., and P. W. Brandt. 1980. Sinusoidal analysis: a high resolution method for correlating biochemical reactions with physiological processes in activated skeletal muscles of rabbit, frog and crayfish. *J. Muscle Res. Cell Motil.* 1:279–303.

Mason, P., and H. Hasan. 1980. Muscle crossbridges in excitation and relaxation. *Experientia (Basel).* 36:949–950.

Mashima, H., and H. Washio, 1968. The changes in membrane potential produced by alternating current or repetitive square pulses in the frog skeletal muscle fibres. *Jpn. J. Physiol.* 18:403–416.

Matsubara, I., and N. Yagi. 1978. A time-resolved x-ray diffraction study of muscle during twitch. *J. Physiol. (Lond.)*. 278:297–307.

Podolsky, R. J., and A. C. Nolan. 1972. Muscle contraction transients, crossbridge kinetics and the Fenn effect. *Cold Spring Harbor Symp. Quant. Biol.* 37:661–668.

Schoenberg, M., and J. B. Wells. 1984. Stiffness, force, and sarcomere shortening during a twitch in frog semitendinosus muscle bundles. *Biophys. J.* 45:389–397.

Schoenberg, M., J. B. Wells, and R. J. Podolsky. 1974. Muscle compliance and the longitudinal transmission of mechanical impulses. *J. Gen. Physiol.* 64:623–642.

Sten-Knudsen, O. 1957. Mechanical response and membrane potential during transverse stimulating of frog muscle. *Acta Physiol. Scand.* 41:132–133.

Tamura, Y., I. Hatta, T. Matsuda, H. Sugi, and T. Tsuchiya. 1982. Changes in muscle stiffness during contraction recorded using ultrasonic waves. *Nature (Lond.)*. 299:631–633.

White, D. C. S., M. M. K. Donaldson, G. E. Pearce, and M. G. A. Wilson. 1977. The resting elasticity of insect fibrillar flight muscle, and properties of the crossbridge cycle. *In* Insect Flight Muscle. R. T. Tregear, editor. North Holland Publishing Company, Amsterdam. 197–208.

Yamamoto, T., and J. W. Herzig. 1978. Series elastic properties of skinned muscle fibres in contraction and rigor. *Pfluegers Arch. Eur. J. Physiol.* 373:21–24.